Volume 48
Number 48
28 December 2024
Pages 20097–20426

NJC

New Journal of Chemistry

A journal for new directions in chemistry

rsc.li/njc

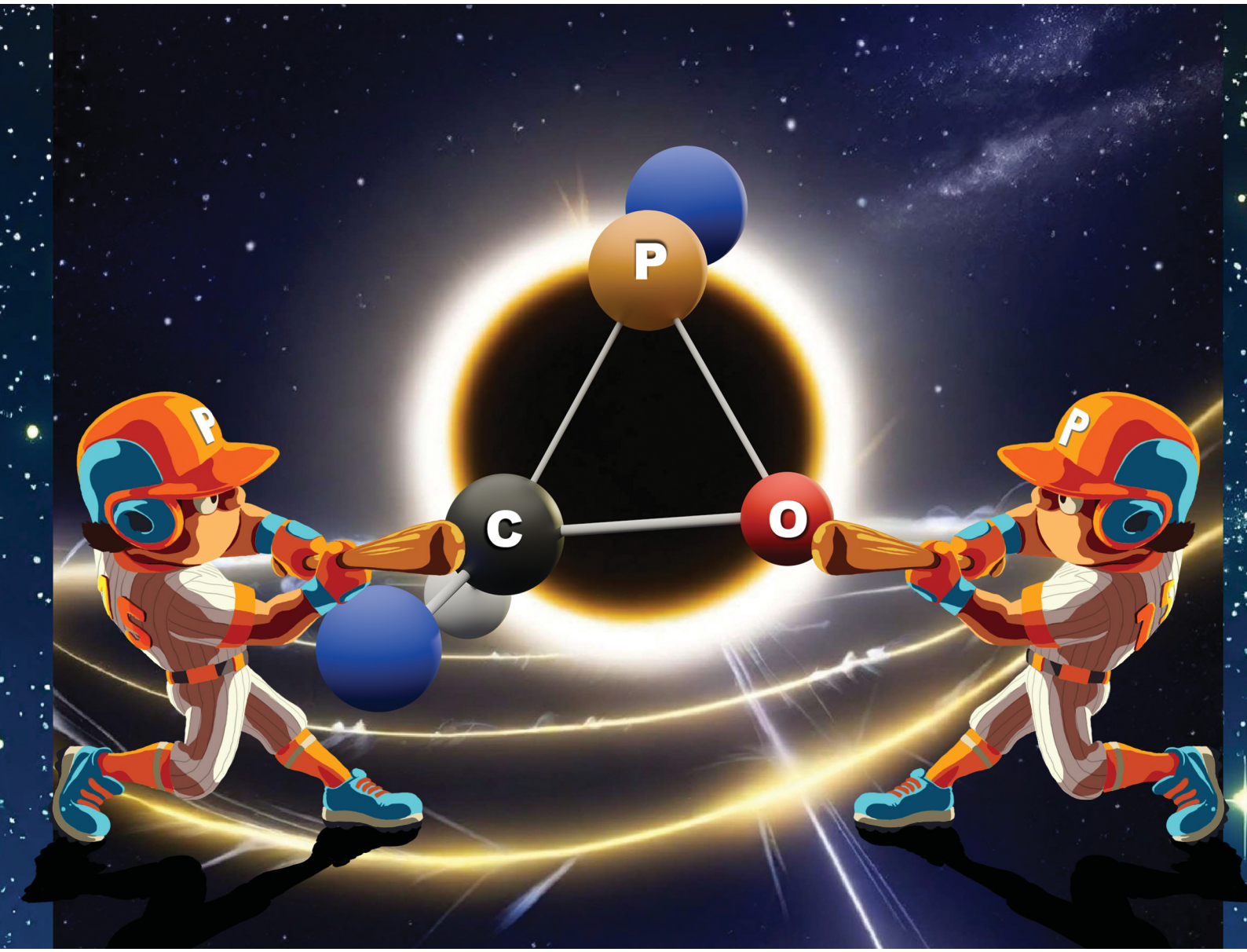

ISSN 1144-0546

ROYAL SOCIETY OF CHEMISTRY

PAPER

Antonio García Alcaraz, Arturo Espinosa Ferao and Rainer Streubel

Computational studies of ring cleavage and deoxygenation reactions of a $\sigma^3\lambda^3$-oxaphosphirane

cnrs

NJC

ROYAL SOCIETY OF CHEMISTRY

PAPER

View Article Online
View Journal | View Issue

Check for updates

Cite this: *New J. Chem.*, 2024, **48**, 20119

Computational studies of ring cleavage and deoxygenation reactions of a $\sigma^3\lambda^3$-oxaphosphirane†

Antonio García Alcaraz, [a] Arturo Espinosa Ferao *[a] and Rainer Streubel *[b]

Received 17th June 2024,
Accepted 21st September 2024

DOI: 10.1039/d4nj02773f

rsc.li/njc

The thermal stability of a $\sigma^3\lambda^3$-oxaphosphirane is computationally explored with regard to their ring-opening reactions. The possibility of deoxygenation by trivalent phosphorus reagents, leading to phosphaalkenes, is found to be disfavoured by direct attack of P to O but, instead, the initial C-attack is kinetically preferred leading to a 1,2,4-oxadiphosphetane *via* the corresponding betaine. Epimerization of this four-membered ring, from the initial *erythro* to the most stable *threo* diastereomeric pair, enables [2+2] cycloreversion to the most stable final *E*-phosphaalkene as the final deoxygenation product.

Open Access Article. Published on 24 September 2024. Downloaded on 5/8/2026 5:03:59 PM.
This article is licensed under a Creative Commons Attribution-NonCommercial 3.0 Unported Licence.

Introduction

The structure and high reactivity of three-membered rings have fascinated both experimental and theoretical chemists over the years.[1] These qualities have led to the synthesis and characterisation of numerous small-sized organic[2] and inorganic[3] heterocycles in recent decades. The high reactivity and instability of these species arises mainly from the high ring strain energy (RSE), which is key, for example, in ring-opening polymerisations of oxiranes and other small-sized rings,[4] and in ring-opening reactions.[5] Oxiranes (epoxides)[6] are of paramount importance in molecular organic and polymer chemistry, but only one example of the heavier three-membered ring analogues oxasiliranes **I**[7] (Fig. 1) was reported so far. Similarly, oxaziridines[8] are versatile organic reagents, but their heavier analogues, $\sigma^3\lambda^3$-oxaphosphiranes **II** are almost unexplored even though, owing to their extraordinary structural and electronic flexibility, organophosphorus compounds are highly versatile reagents with a fundamental role in today's synthetic chemistry.[9] Part of their structural versatility may be considered to derive from their diagonal analogy in the periodic table with carbon, which led to the coining of the expression *'Phosphorus: the carbon copy'*.[10] On the contrary, *P*-ligated versions of oxaphosphiranes **III**[11] are firmly established since the early discover by Mathey using epoxidation of phosphaalkene *P*-complexes,[12] the phosphinidene complex transfer reaction to carbonyls[13] and the most recent and convenient protocol using Li/Cl-phosphinidenoid complexes.[14] Also, $\sigma^5\lambda^5$-oxaphosphiranes **IV** derivatives have been known for a long time as unstable intermediates in the reaction of alkyl phosphites or phosphanes with carbonyl compounds, earlier proposed by Perkow,[15] Ramirez,[16] Mironov[17] and, theoretically, later by Espinosa Ferao.[18] Only in one case, reported by Barrans,[19] a ^{31}P-NMR signal at −25 ppm was attributed to a type **IV** intermediate, but without providing further analytical data. Even a $\sigma^4\lambda^5$-oxaphosphirane *P*-imide **V** was prepared from iminophosphanes and fluorinated ketones.[13a] Recently, the first example of an unligated $\sigma^3\lambda^3$-oxaphosphirane **II** was prepared by decomplexation of a κ*P*-pentacarbonylmolybdenum(0) complex **III** using bis(diphenylphosphino)ethane (DPPE), and only adduct formation with borane and various reactions under oxidative conditions were explored.[20] Even more recently, the decomplexation was most conveniently achieved with *N*-methyl imidazole and a wider set of reactions thoroughly studied showing an interesting reactivity feature of the P fragment behaving as a formal singlet phosphinidene, albeit being still part of the ring.[21]

Several preliminary theoretical studies on oxaphosphiranes have already highlighted the ease of *P*-complexation[22] and their high ring strain energy (RSE).[23] Indeed, strained small heterocycles are prone to undergoing ring-opening reactions by the action of external initiators, as occurs at the heart of oxirane chemistry[6] and as has also been shown recently with very

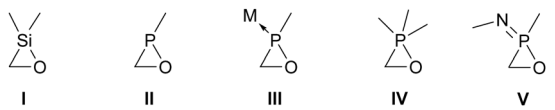

I II III IV V

Fig. 1 Heavier group 14 and 15 three-membered rings, including those with higher coordination at phosphorus; external lines denote organic substituents.

[a] *Departamento de Química Orgánica, Facultad de Química, Universidad de Murcia, Campus de Espinardo, 30071, Spain. E-mail: artuesp@um.es*
[b] *Intitut für Anorganische Chemie, Rheinische Friedrich-Wilhelms-Universität Bonn, Gerhard-Domagk-Str. 1, 53121 Bonn, Germany. E-mail: r.streubel@uni-bonn.de*

† Electronic supplementary information (ESI) available: Cartesian coordinates and energies for all computed species. See DOI: https://doi.org/10.1039/d4nj02773f

Open Access Article. Published on 24 September 2024. Downloaded on 5/8/2026 5:03:59 PM.
This article is licensed under a Creative Commons Attribution-NonCommercial 3.0 Unported Licence.

simple model oxaphosphiranes.[23b] The latter have revealed their potential to also undergo closed-shell isomerisation reactions by breaking one of their endocyclic bonds, with preferential cleavage of the endocyclic C–O bond over the P–C bond.[24] In addition, the recent report on the PZ_3 reagent-promoted deoxidation of oxiranes to alkenes[25] makes oxaphosphiranes an interesting potential source of phosphaalkenes.

Herein, theoretical results on endocyclic bond cleavage processes and reactions of an unligated 3,5-difluorophenyl-substituted oxaphosphirane towards P(III) reagents are reported.

Results and discussion

A simplified model of a potentially accessible derivative bearing a *tert*-butyl group as a *P*-substituent and the experimentally used 3,5-difluorophenyl group as a *C*-substituent[21] (**1**) was chosen to explore the thermal stability of the ring by looking at the cleavage processes of the three endocyclic bonds (Scheme 1). The cleavage of the C–O bond exergonically produced the open-chain $\sigma^3\lambda^5$-isomer phosphaalkene *P*-oxide **2** in a kinetically favoured process (Fig. 2). Phosphaalkene *P*-oxides (alkylidene(oxo)phosphoranes) are phospha-analogues of nitrones[26] (imine *N*-oxides), that are useful intermediates in chemical synthesis and formally derived from C–O cleavage in the much more strained oxaziridine rings (computed RSE = 26.4 kcal mol^{-1} for the parent ring).[27] This isomer **2** is stable towards dissociation (after intersystem crossing, ISC) into the triplet carbene $\mathbf{3^t}$ and *tert*-butyl phosphinidene oxide **4**. In contrast, cleavage of the P–C bond gave rise to the zwitterionic species **5** in an endergonic process with a moderately high activation barrier (34.5 kcal mol^{-1}). Although not experimentally observed so far in free oxaphosphiranes, the related C–O and P–C bond cleavage processes constitute the initial step in many reactions displayed by their κ-*P*-complexes.[28] The less favoured ring opening process was found to be the P–O bond cleavage leading to the endergonic dissociation into aldehyde **6** and triplet state phosphinidene $\mathbf{7^t}$ (Fig. 2), with high

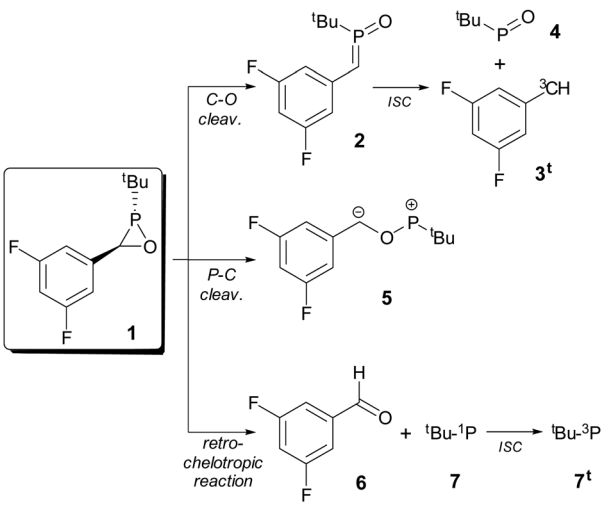

Scheme 1 Studied ring-opening reactions from oxaphosphirane **1**.

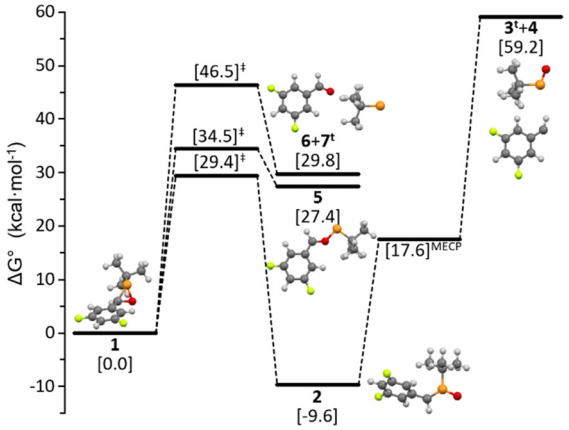

Fig. 2 Computed (CPCM(tol)/PWPB95-D3/def2-QZVPP) relative Gibbs free energy profile for endocyclic bond cleavage processes in **1**.

intersystem crossing energy. The first step is very much related to the observed singlet phosphinidene-like reactivity of the oxaphosphirane P fragment.[21] These results show that oxaphosphirane **1** is stable towards the cleavage of its P–C and P–O bonds, but the most labile C–O bond only displays significant kinetic protection ($\Delta G^{\ddagger}$ = 29.4 kcal mol^{-1}).

Next, the reaction of **1** with different trivalent phosphorus compounds (PMe_3, $P(OMe)_3$ and $P(NMe_2)_3$) **8a–c** was explored. First, the abstraction of the O atom from oxaphosphirane **1** by the P(III) reagent was studied, leading to the formation of phosphane oxides **9** and phosphaalkene $\mathbf{10}^{E}$, owing to the assumed *trans* stereochemistry of the starting oxaphosphirane (Scheme 2). According to the very recent published work on the deoxygenation of oxiranes,[25] it seems reasonable to posit that this reaction occurs by direct nucleophilic attack of the phosphorus centre of the PZ_3 reagent to the O atom of oxaphosphirane **1**. The values reported in the aforementioned work on *Thermodynamic Oxygen atom transfer Potentials* (TOP^{H}, the superscript 'H' referring to the use of enthalpies for energy evaluation) allow for predictions. Here, three PZ_3 reagents were tested, PMe_3 **8a** (TOP^{H} = −100.1 kcal mol^{-1}), $P(OMe)_3$ **8b** (TOP^{H} = −113.9 kcal mol^{-1}), and $P(NMe_2)_3$ **8c** (TOP^{H} = −111.1 kcal mol^{-1}), and they should be able to deoxygenate oxaphosphiranes, which are the oxidized species of the redox couple with the corresponding phosphaalkene (TOP^{H} = −63.7 kcal mol^{-1} reported for 2,2,2-trimethyloxaphosphirane).[27,29] Indeed, at the calculation level used in this work (CPCM(tol)/PWPB95-D3/def2-QZVPP), a TOP^{H} of −73.1 kcal mol^{-1} has been estimated for the $\mathbf{10}^{E}$/**1** redox pair and −99.6, −109.0 and −110.1 kcal mol^{-1} for the **8**/**9** redox pairs for PMe_3, $P(OMe)_3$ and $P(NMe_2)_3$, respectively, *versus* the H_2O/H_2O_2 pair used as a reference. Consistent with these TOP^{H} oxophilicity parameters, and the difference ΔTOP^{H} = −26.5, −35.9 and −37.1 kcal mol^{-1} for PMe_3, $P(OMe)_3$ and $P(NMe_2)_3$, respectively, markedly exergonic values have been obtained for the deoxygenation of **1** (ΔG = −31.8, −38.7 and −40.8 kcal mol^{-1}, respectively), with very energetic transition states, the kinetically most favourable case being that of PMe_3 (Scheme 2). These results demonstrate that the use of the

 This journal is © The Royal Society of Chemistry and the Centre National de la Recherche Scientifique 2024

Open Access Article. Published on 24 September 2024. Downloaded on 5/8/2026 5:03:59 PM.
This article is licensed under a Creative Commons Attribution-NonCommercial 3.0 Unported Licence.

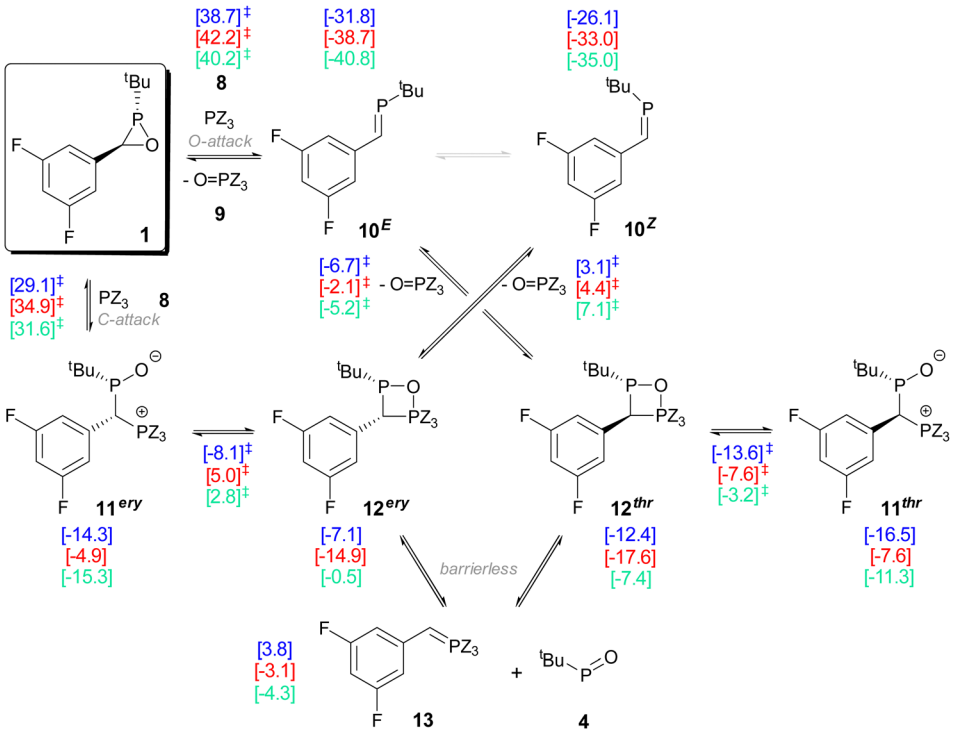

Scheme 2 Computed (CPCM(tol)/PWPB95-D3/def2-QZVPP) pathways in the reaction of **1** with phosphanes **8**. Relative Gibbs free energies (kcal mol^{-1}) in square brackets and colour coded according to the phosphane used: blue (**8a**), red (**8b**) and green (**8c**).

phosphorus compounds PMe_3, $P(OMe)_3$ and $P(NMe_2)_3$ to form phosphaalkenes from oxaphosphiranes could be experimentally feasible, but only under very harsh conditions.

Approach of the P(III) reagent **8** to oxaphosphirane **1** takes places by interacting the basic P centre of **8** with one of the two lobes of the LUMO, mostly located at a phosphorus p-type atomic orbital, of **1**,[21] and leading to an encounter complex **1·8**.

Taking PMe_3 as a case in point, its interaction with **1** can be predicted using DFT-rooted parameters[30] related with Pearson theory of hard and soft acids and bases (HSAB).[31] The (local) quadratic difference in softness $(\Delta S)^2$ is much lower for the interaction with the ring P atom (0.14) than with the O (1.62) or C (1.96) ring atoms. Also, the initial interaction energy ΔE_{int}, resulting from two-step sequential chemical potential-equalization and reshuffling of the charge distribution,[32] points to a most favourable initial interaction with P over O and C (−87.1, −42.5 and −40.9 kcal mol^{-1}, respectively). Indeed, the attack of **8a** to the O atom of **1** to promote deoxygenation was found to required formation of the encounter complex **1·8a$^{(O)}$** with rather exothermic P···P interaction (ΔE_{ZPE} = −23.6 kcal mol^{-1}, ΔG_{rel} = 8.4 kcal mol^{-1}). However, another similar most stable encounter complex **1·8a$^{(C)}$** was found at the C-side of the ring (ΔE_{ZPE} = −25.7 kcal mol^{-1}, ΔG_{rel} = 7.1 kcal mol^{-1}). Both initial species **1·8a** display a P···P pattern corresponding to a van der Waals complex according to a recent definition,[33] on the basis of the small positive value of Laplacian of the electron density at the bond critical points (BCPs) and the relative position of the donor (P_D) and acceptor (P_A) valence-shell charge concentration (VSCC) bands at both sides of the BCP (Fig. 3).[33b]

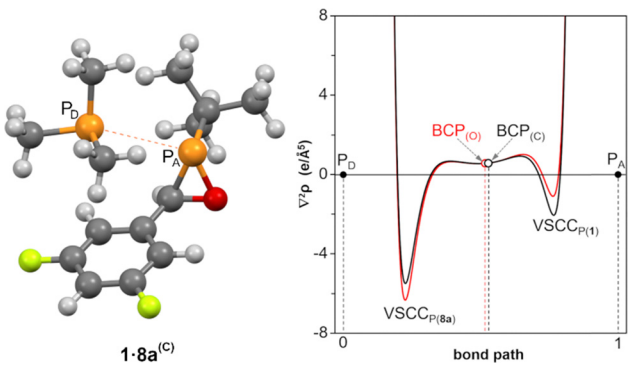

Fig. 3 Computed (B3LYP/def2-TZVPP//CPCM(tol)/PBEh-3c) structure of van der Waals complex **1·8a$^{(C)}$** and variation of the Laplacian of the electron density along the P···P bond path for **1·8a$^{(C)}$** (black) and **1·8a$^{(O)}$** (red).

The alternative reaction of the phosphorus attack of the PZ_3 reagent **8** at the ring C atom of the oxaphosphirane **1** starts from the van der Waals complex **1·8$^{(C)}$** and gives rise to the zwitterionic species (betaines) **11^{ery}** (Scheme 2). Compared to *O*-abstraction, this process is thermodynamically less favourable, although the activation barriers are noticeably smaller, making them the kinetic products of reactions with PZ_3. These betaines can cyclise to the corresponding 1,2,4-oxadiphosphetanes **12^{ery}** through a process with low activation barrier, which in turn, may undergo a [2+2] cycloreversion producing the elimination of the phosphane oxide O=PZ_3 (**9**) and leading exergonically to

Open Access Article. Published on 24 September 2024. Downloaded on 5/8/2026 5:03:59 PM.
This article is licensed under a Creative Commons Attribution-NonCommercial 3.0 Unported Licence.

a phosphaalkene, the product of the oxaphosphirane **1** deoxygenation, but now with the opposite *Z*-configuration (**10**^{Z}). In the case of oxiranes, also the attack of PZ_3 to the O atom (deoxygenation) is less favoured than to the ring C atom but, in the latter case, carbene transfer with the elimination of the carbonyl component ($PZ_3 \rightarrow R_2C = PZ_3$) usually occurs due to the low stability of the betaine C–C bond.[25] The other possible [2+2] cycloreversion in *erythro* 1,2,4-oxadiphosphetanes **12**^{ery} leads to phosphorane **13** and phosphinidene oxide **4**. A variety of [2+2] cycloreversion reactions in related 1,2-oxaphosphetanes with the P centre in different oxidation states and coordination numbers have recently been reported,[34] the $\sigma^5\lambda^5$-P centre being the most favoured for P=O bond formation. Recombination of **13** and **4** through the opposite molecular face in one of the reagents would give rise to the diastereomeric 1,2,4-oxadiphosphetane **12**^{thr}, hence opening the path to phosphaalkene **10**^{E} by loss of phosphane oxide **9** (Scheme 2). All herein studied [2+2] cycloreversion reactions of 1,2,4-oxadiphosphetanes **12** affording phosphorane **13** and phosphinidene oxide **4** were found to be barrierless processes.

Using the reaction of **1** with PMe_3 (**8a**) as a case in point, the latter behaves as a nucleophile as demonstrated by the (Mulliken) electric charge transferred from the phosphane to the oxaphosphirane in the TS for both the O- ($\Delta q^{M} = 0.31e$) and C-attack ($\Delta q^{M} = 0.25e$). The initial betaine formation (**1** + **8a** → **11a**^{ery}) is the rate-determining step, all subsequent steps having lower activation barriers (Fig. 4) which would lead to the formation of the most stable *E*-phosphaalkene (**10**^{E}). The *Z*-isomer **10**^{Z} would be formed somewhat faster, following a slightly lower energy profile, but the activation energy for the reverse reaction (**10**^{Z} + **9a** → **12a**^{ery}) is almost identical to that of the initial step (Fig. 4). Hence, in the required thermal regime all the subsequent steps could reach equilibrium and thus favour the overall preferential formation of the more stable phosphaalkene **10**^{E}. As expected, cleavage of both diastereomeric 1,2,4-oxadiphosphetanes (**12a**) to the corresponding phosphaalkene (**10**) occurs through less stable intermediately formed isomers with the ring O atom in the equatorial position around the trigonal bipyramidal $\sigma^5\lambda^5$-P atom (**12a**$^{-eq}$). Worth mentioning is that the regioselectivity of the [2+2] cycloaddition of **13a** and **4** can be explained in terms of the lower quadratic difference in local softness (2.99) compared to the other (not shown) interaction that would lead to regioisomer 1,2,3-oxadiphosphetane (6.47).

In the case of the reaction of $P(OMe)_3$ (**8b**) with **1** (Fig. 5), although the potential energy surface is qualitatively similar, excepting the higher barrier for the initial rate-determining step, formation of the *Z*-phosphaalkene from the initially produced 1,2,4-oxadiphosphetanes (**12b**^{ery}) is kinetically disfavoured compared to the alternative [2+2] cycloreversion affording **13b** and **4**, which in turn opens the lower energy pathway finally leading to the most stable *E*-phosphaalkene **10**^{E} (Fig. 5). No *O*-equatorial isomers were found for these 1,2,4-oxadiphosphetanes **12b**, but three different rotamers for the *P*-methoxy substituents were located for each diastereomer.

Finally, when the phosphorus reagent is $P(NMe_2)_3$, the activation energies for both possible pathways are in between those of the reactions with PMe_3 and $P(OMe)_3$ and following the same preference for the attack to the ring C atom over the O atom attack (Fig. 6). In this case, the initially formed *erythro* 1,2,4-oxadiphosphetane **12c**^{ery} is rather destabilized and is converted into the most stable *threo* isomer **12c**^{thr} through two consecutive barrierless [2+2] cycloreversion and [2+2] cycloaddition steps, hence enabling the preferential formation of the most stable *E*-phosphaalkene **10**^{E} (Fig. 6).

Moreover, the reductive potential reported for the unsubstituted $\sigma^3\lambda^3$-oxaphosphirane itself ($TOP^{H} = -90.6$ kcal mol^{-1}),[25] to be converted into the corresponding *P*-oxide, must be sufficient to deoxygenate the oxaphosphirane ring (*vide supra*). Indeed, at the working level of theory, the TOP^{H} for the **1**/**14** pair is −93.8 kcal mol^{-1} and the disproportionation of two molecules of **1** to give **10**^{E} and the corresponding oxaphosphirane *P*-oxide **14** was computed to be exergonic by $\Delta G = -23.8$ kcal mol^{-1}.

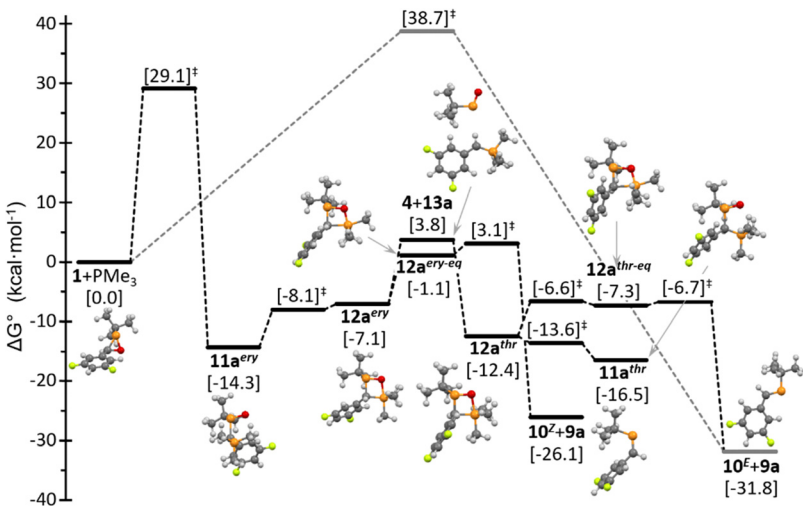

Fig. 4 Computed (CPCM(tol)/PWPB95-D3/def2-QZVPP) relative free Gibbs energy profile for the reaction of **1** with PMe_3.

 This journal is © The Royal Society of Chemistry and the Centre National de la Recherche Scientifique 2024

Open Access Article. Published on 24 September 2024. Downloaded on 5/8/2026 5:03:59 PM.
This article is licensed under a Creative Commons Attribution-NonCommercial 3.0 Unported Licence.

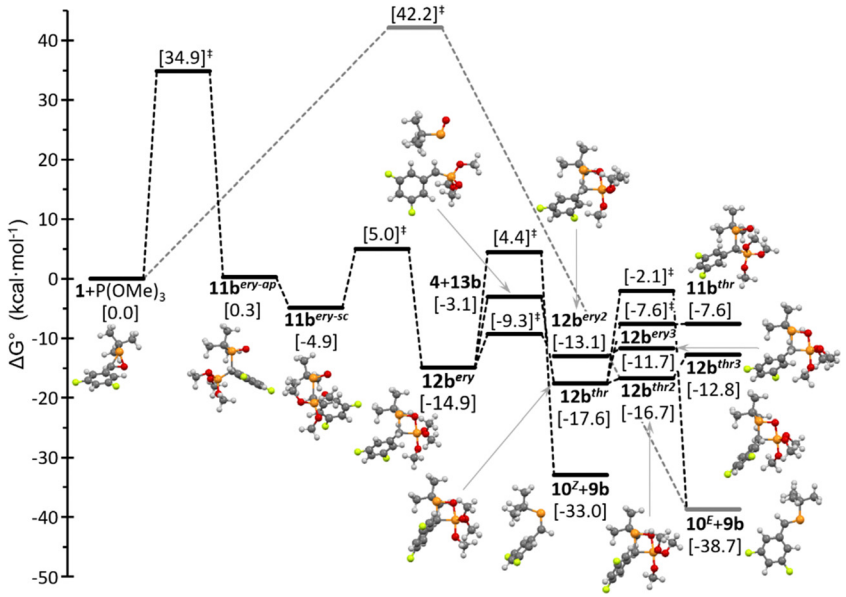

Fig. 5 Computed (CPCM(tol)/PWPB95-D3/def2-QZVPP) relative free Gibbs energy profile for the reaction of **1** with $P(OMe)_3$.

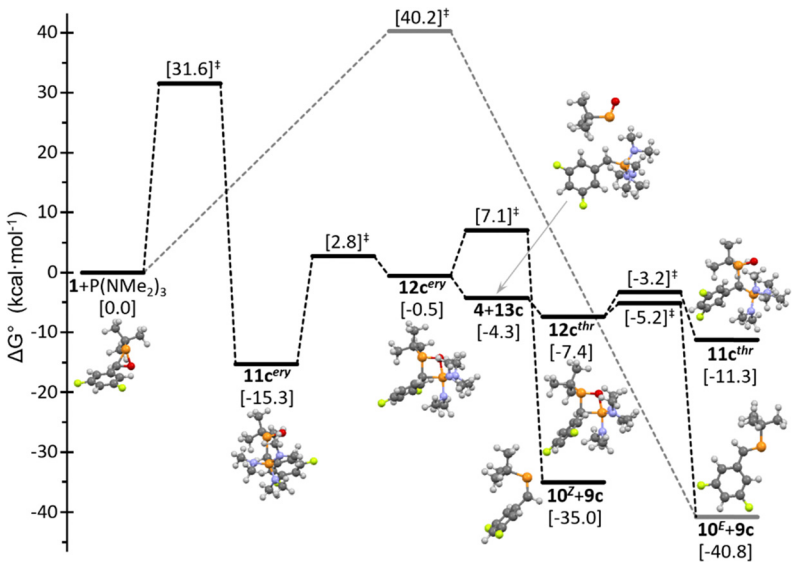

Fig. 6 Computed (CPCM(tol)/PWPB95-D3/def2-QZVPP) relative free Gibbs energy profile for the reaction of **1** with $P(NMe_2)_3$.

Computational methods

DFT calculations were performed with the ORCA electronic structure program package (version 4.2.1).[35] All geometry optimizations were run in redundant internal coordinates with tight convergence criteria, in the gas phase and using Grimme's dispersion-corrected composite PBEh-3c level.[36] For the mechanistic studies (*i.e.*, excluding TOP^H evaluations that were computed in the gas phase), solvent (toluene) effects were taken into consideration with the CPCM solvation method,[37] as implemented in ORCA. Harmonic frequency calculations at the optimization level were used to obtain thermal correction contributions and verified the nature of ground or transition states (TS) having all positive frequencies or only one imaginary frequency, respectively. TS structures were further confirmed by following the intrinsic reaction path in both directions of the negative eigenvector. Final energies were obtained by means of single-point energy calculations with the double-hybrid-meta-GGA functional PWPB95,[38] the Grimme's semiempirical D3 correction[39] and the def2-QZVPP basis set,[40] using the RI-JK approximation.[41] The topological analysis was performed with the electron density at B3LYP/def2-TZVPP and using the Multiwfn program.[42]

Conclusions

The stability of the $\sigma^3\lambda^3$-oxaphosphirane ring system towards thermal ring cleavage was theoretically explored for

Open Access Article. Published on 24 September 2024. Downloaded on 5/8/2026 5:03:59 PM.
This article is licensed under a Creative Commons Attribution-NonCommercial 3.0 Unported Licence.

trans-3-(3,5-difluorophenyl)-2-*tert*-butyl-oxaphosphirane. Only the C–O bond cleavage is slightly exergonic (ΔG = −9.6 kcal mol^{-1}) and proceeds over a moderate barrier ($\Delta G^{\ddagger}$ = 29.4 kcal mol^{-1}).

Reaction of this derivative with P(III)-reagents leading to a deoxygenation (P → O attack) is always kinetically disfavoured (by 7.3–9.6 kcal mol^{-1}). The preferred P → C attack is the rate-limiting step of the stepwise, alternative deoxygenation involving betaine formation, and a ring-closure to give an *erythro*-1,2,4-oxadiphosphetane, while [2+2]-cycloreversion affords the less stable *Z*-configured phosphaalkene. The stable *E*-phosphaalkene derivative can be easily accessed through the barrierless alternative oxadiphosphetane [2+2]-cycloreversion which opens the path to the [2+2]-cycloaddition to yield the *threo* diastereomer. In the thermal conditions required for overcoming the first rate-limiting step, the equilibrium conditions should favour the formation of the most stable *E*-phosphaalkene as the major final product. Further mechanistic investigations on the thermodynamically favoured oxaphosphirane disproportionation leading to a phosphaalkene and an oxaphosphirane *P*-oxide are currently ongoing.

Author contributions

A. E. F. and R. S. are responsible for the conceptualization. A. G. A. and A. E. F. performed all calculations, data analysis and wrote the ESI.† All authors contributed to writing the manuscript from the first draft.

Data availability

The data supporting this article have been included as part of the ESI.†

Conflicts of interest

There are no conflicts to declare.

Acknowledgements

The authors are thankful for the computational resources used at the computation centre at *Servicio de Cálculo Científico* (SCC – University of Murcia).

Notes and references

1 (*a*) D. Cremer and E. Kraka, *J. Am. Chem. Soc.*, 1985, **107**, 3800–3810; (*b*) J. A. Boatz and M. S. Gordon, *J. Phys. Chem.*, 1989, **93**, 3025–3029; (*c*) A. Skancke, D. Van Vechten, J. F. Liebman and P. N. Skancke, *J. Mol. Struct.*, 1996, **376**, 461–468; (*d*) M. Alcamí, O. Mó and M. Yáñez, *J. Comput. Chem.*, 1998, **19**, 1072–1086; (*e*) T. P. M. Goumans, A. W. Ehlers, K. Lammertsma and E.-U. Würthwein, *Eur. J. Org. Chem.*, 2003, 2941–2946.

2 A. Hassner, *The Chemistry of Heterocyclic Compounds, Small Ring Heterocycles*, Wiley, 2009.

3 G. He, O. Shynkaruk, M. W. Lui and E. Rivard, *Chem. Rev.*, 2014, **114**, 7815–7880.

4 (*a*) P. Kubisa, *J. Polym. Sci., Part A: Polym. Chem.*, 2003, **41**, 457–468; (*b*) I. C. Stewart, C. C. Lee, R. G. Bergman and F. D. Toste, *J. Am. Chem. Soc.*, 2005, **127**, 17616–17617.

5 C.-Y. Huang and A. G. Doyle, *Chem. Rev.*, 2014, **114**, 8153–8198.

6 (*a*) A. Wurtz, *Comptes Rendus*, 1859, **48**, 101–105; (*b*) L. G. Wade Jr. and J. W. Simek, *Organic Chemistry*, Pearson Education Ltd, Essex, England, 9th edn, 2017.

7 D. Gau, R. Rodriguez, T. Kato, N. Saffon-Merceron, F. P. Cossío and A. Baceiredo, *Chem. – Eur. J.*, 2010, **16**, 8255–8258.

8 K. S. Williamson, D. J. Michaelis and T. P. Yoon, *Chem. Rev.*, 2014, **114**, 8016–8036.

9 (*a*) *Organophosphorus Reagents in Organic Synthesis*, ed. J. I. G. Cadogan, Academic Press, London, New York, 1979; (*b*) R. Engel, *Handbook of Organophosphorus Chemistry*, CRC Press, 1992; (*c*) P. Savignac and B. Iorga, *Modern Phosphonate Chemistry*, CRC Press, 2003; (*d*) P. J. Murphy, *Organophosphorus Reagents: A Practical Approach in Chemistry, Practical Approach in Chemistry*, 2004.

10 K. B. Dillon, F. Mathey and J. F. Nixon, *Phosphorus: The Carbon Copy. From Organophosphorus to Phospha-organic Chemistry*, Wiley, 1998.

11 N. Volk, P. Malik, A. García Alcaraz, A. Espinosa Ferao and R. Streubel, *Coord. Chem. Rev.*, 2021, **437**, 213818.

12 S. Bauer, A. Marinetti, L. Ricard and F. Mathey, *Angew. Chem., Int. Ed.*, 1990, **29**, 1166–1167.

13 (*a*) G.-V. Röschenthaler, K. Sauerbrey and R. Schmutzler, *Chem. Ber.*, 1978, **111**, 3105–3111; (*b*) E. Niecke, D. Gudat, W. W. Schoeller and P. Rademacher, *J. Chem. Soc., Chem. Commun.*, 1985, 1050–1051; (*c*) F. U. Seifert and G.-V. Röschenthaler, *Z. Naturforsch., B: Chem. Sci.*, 1993, **48**, 1089–1093; (*d*) R. Streubel, A. Kusenberg, J. Jeske and P. G. Jones, *Angew. Chem., Int. Ed. Engl.*, 1995, **33**, 2427–2428; (*e*) R. Streubel, N. Volk, G. Schnakenburg, A. García Alcaraz and A. Espinosa Ferao, *Eur. J. Inorg. Chem.*, 2021, 252–257.

14 A. Schmer, P. Junker, A. Espinosa Ferao and R. Streubel, *Acc. Chem. Res.*, 2021, **54**, 1754–1765.

15 (*a*) W. Perkow, K. Ullerich and F. Meyer, *Naturwissenschaften*, 1952, **39**, 353; (*b*) W. Perkow, *Chem. Ber.*, 1954, **87**, 755–758.

16 F. Ramirez, P. C. Smith, J. F. Pilot and A. S. Gulati, *J. Org. Chem.*, 1968, **33**, 3787–3794.

17 (*a*) R. M. Aminova, V. F. Mironov, M. E. Filatov and L. I. Savostina, *Zh. Obshch. Khim.*, 1996, **66**, 1042; (*b*) R. M. Aminova, V. F. Mironov and M. E. Filatov, *Zh. Obshch. Khim.*, 1999, **69**, 58; (*c*) R. M. Aminova, G. A. Shamov, V. N. Mushkin, V. F. Mironov, A. I. Konovalov and A. V. Aganov, *Phosphorus, Sulfur Silicon Relat. Elem.*, 1999, **147**, 265.

18 (*a*) A. Espinosa Ferao, *J. Phys. Chem. A*, 2017, **121**, 6517–6522; (*b*) A. Espinosa Ferao, *Inorg. Chem.*, 2018, **57**(14), 8058–8064.

 This journal is © The Royal Society of Chemistry and the Centre National de la Recherche Scientifique 2024

Open Access Article. Published on 24 September 2024. Downloaded on 5/8/2026 5:03:59 PM. This article is licensed under a Creative Commons Attribution-NonCommercial 3.0 Unported Licence.

19 M. T. Boisdon and J. Barrans, *J. Chem. Soc., Chem. Commun.*, 1988, 615–617.
20 J. Faßbender, N. Volk, A. García Alcaraz, S. Balasubramaniam, A. Espinosa Ferao and R. Streubel, *Chem. Commun.*, 2023, **59**(10), 1285–1288.
21 N. Volk, A. García Alcaraz, S. Balasubramaniam, Y. Heumann, G. Schnakenburg, A. Espinosa Ferao and R. Streubel, *Chem. Sci.*, submitted (ID SC-EDG-09-2024-006185).
22 A. Espinosa, E. de las Heras and R. Streubel, *Inorg. Chem.*, 2014, **53**, 6132–6140.
23 (*a*) O. Krahe, F. Neese and R. Streubel, *Chem. – Eur. J.*, 2009, **15**, 2594–2601; (*b*) A. Espinosa Ferao, A. Rey Planells and R. Streubel, *Eur. J. Inorg. Chem.*, 2021, 348–353.
24 A. Espinosa Ferao and R. Streubel, *Eur. J. Inorg. Chem.*, 2017, 2707–2712.
25 A. Espinosa Ferao, *ChemPlusChem*, 2024, **89**, e202300474.
26 (*a*) J. Hamer and A. Macaluso, *Chem. Rev.*, 1964, **64**(4), 473–495; (*b*) G. R. Delpierre and M. Lamchen, *Chem. Soc. Rev.*, 1965, **19**(4), 329–348.
27 A. Rey Planells and A. Espinosa Ferao, *Chem. – Eur. J.*, 2023, **29**, e202302243.
28 (*a*) R. Streubel, C. Murcia-García, G. Schnakenburg and A. Espinosa Ferao, *Organometallics*, 2015, **34**, 2676–2682; (*b*) M. Klein, G. Schnakenburg, A. Espinosa Ferao and R. Streubel, *Dalton Trans.*, 2016, **45**, 2085–2094; (*c*) C. Murcia García, A. Espinosa Ferao, G. Schnakenburg and R. Streubel, *Dalton Trans.*, 2016, **45**, 2378–2385; (*d*) P. Malik, A. Espinosa Ferao, G. Schnakenburg and R. Streubel, *Angew. Chem., Int. Ed.*, 2016, **55**, 12693–12697; (*e*) J. Faßbender, G. Schnakenburg, A. Espinosa Ferao and R. Streubel, *Dalton Trans.*, 2018, **47**, 9347–9354.
29 It should be noted that the above displayed values for PMe_3 and $P(NMe_2)_3$ do not correspond to those previously reported (TOP^H = −97.0 and −43.2 kcal mol^{-1}, respectively) and, therefore, were recalculated in the present work.
30 (*a*) R. G. Parr and W. Yang, in *Density-functional theory of atoms and molecules*, Oxford University Press, New York, 1989; (*b*) R. G. Parr and R. G. Pearson, *J. Am. Chem. Soc.*, 1983, **105**, 7512–7516; (*c*) J. L. Gázquez, in *Chemical Hardness*, ed. K. D. Sen, *Struct. Bonding*, 1993, **80**, pp. 27–43.
31 (*a*) R. G. Pearson, *J. Am. Chem. Soc.*, 1963, **85**, 3533–3539; (*b*) T. L. Ho, *Chem. Rev.*, 1975, **75**, 1–20.
32 (*a*) P. K. Chattaraj, H. Lee and R. G. Parr, *J. Am. Chem. Soc.*, 1991, **113**, 1855–1856; (*b*) R. G. Parr and J. L. Gázquez, *J. Phys. Chem.*, 1993, **97**, 3939–3940.
33 (*a*) M. W. Stanford, J. I. Schweizer, M. Menche, G. S. Nichol, M. C. Holthausen and M. J. Cowley, *Angew. Chem., Int. Ed.*, 2019, **58**, 1329; (*b*) A. Espinosa Ferao, A. García Alcaraz, S. Zaragoza Noguera and R. Streubel, *Inorg. Chem.*, 2020, **59**, 12829; (*c*) V. Nesterov, R. Baierl, F. Hanusch, A. Espinosa Ferao and S. Inoue, *J. Am. Chem. Soc.*, 2019, **141**, 14576.
34 A. W. Kyri, F. Gleim, A. García Alcaraz, G. Schnakenburg, A. Espinosa Ferao and R. Streubel, *Chem. Commun.*, 2018, **54**, 7123–7126.
35 F. Neese, *Wiley Interdiscip. Rev.: Comput. Mol. Sci.*, 2012, **2**, 73–78.
36 S. Grimme, J. G. Brandenburg, C. Bannwarth and A. Hansen, *J. Chem. Phys.*, 2015, **143**, 54107.
37 V. Barone and M. Cossi, *J. Phys. Chem. A*, 1998, **102**, 1995–2001.
38 (*a*) L. Goerigk and S. Grimme, *J. Chem. Theory Comput.*, 2011, **7**, 291–309; (*b*) L. Goerigk and S. Grimme, *Phys. Chem. Chem. Phys.*, 2011, **13**, 6670–6688.
39 (*a*) S. Grimme, J. Antony, S. Ehrlich and H. Krieg, *J. Chem. Phys.*, 2010, **132**, 154104–154119; (*b*) S. Grimme, S. Ehrlich and L. Goerigk, *J. Comput. Chem.*, 2011, **32**, 1456–1465.
40 F. Weigend and R. Ahlrichs, *Phys. Chem. Chem. Phys.*, 2005, **7**, 3297–3305.
41 F. Weigend, *J. Comput. Chem.*, 2008, **29**, 167–175.
42 *Multiwfn, v. 3.8*; T. Lu and F. Chen, *J. Comput. Chem.*, 2012, **33**, 580–592Website: **https://sobereva.com/multiwfn/**.